Engineering Transactions, **67**(4): 475–489, 2019, doi: 10.24423/EngTrans.974.20190725
Polish Academy of Sciences • Institute of Fundamental Technological Research (IPPT PAN)
Université de Lorraine • Poznan University of Technology

Research Paper

A Sliding Mode Controller Design for Thermal Comfort in Buildings

Paweł SKRUCH, Marek DŁUGOSZ*

AGH University of Science and Technology
Faculty of Electrical Engineering, Automatics, Computer Science and Biomedical Engineering
Department of Automatic Control and Robotics
Al. Mickiewicza 30, 30-059 Kraków, Poland
*Corresponding Author e-mail: mdlugosz@agh.edu.pl

One of the factors determining comfort in buildings is the indoor air temperature of the rooms. A control system, part of the home automation system, should stabilise air temperature to the desired level, despite various disturbances such as the presence of random or occasional sources of heat. Inaccurate models of the dynamics of air temperature changes in buildings prescribe the use of robust control methods, a type of which is the sliding mode controller. This article presents the application of a sliding mode controller (SMC) to home automation systems, designed to control air temperature inside a building. The sliding-mode controller makes use of sliding surfaces, which are defined by the assumed trajectory and the system output. The control law is designed in such a way that the trajectory of the system tends to the sliding surface from any initial point and remains on it after reaching the sliding surface. In this article, a model at air temperature change dynamics inside a building is presented. The modelling approach relies on the lumped-parameter methodology, in which distributed physical properties are represented by lumped parameters (such as thermal capacity or resistance). The model takes into account the loss of heat through conduction and ventilation, as well as internal heat gain. The parameters of the model can be obtained easily from the thermal properties of the construction materials. Theoretical considerations were applied in simulation experiments and the results of these experiments confirm the performance improvement achieved by the proposed solutions.

Key words: control systems design; sliding-mode control; building temperature dynamics; sliding surface.

1. Introduction

The sliding mode control (SMC) is a robust method that can be successfully used for the control of non-linear and linear systems [1, 2]. The SMC is characterised by the fact that the structure of the control system may vary during the control process. This type of control method is widely used in different applications such as power transmission [3], position control [4] and anti-lock braking system [5]. In this method, first of all, a proper sliding surface is defined [6] and, then, a controller is designed aimed at deriving the system states to the defined sliding (or switching) surface. One of the most notable features of the sliding mode control is that after reaching the sliding mode, the closed-loop system is stable against model parameter variations and external disturbances. The sliding mode control can be designed in two types. Firstly, the linear sliding control mode can be used for the asymptotic stabilisation of the closed-loop system. This controller guarantees that the system state will reach the equilibrium point in infinite time [1]. Secondly, the terminal sliding mode control is based on non-linear, non-smooth differential equations and enables finite time convergence to the equilibrium [7, 8]. In this paper, a modification of the terminal sliding mode controller proposed in [9] has been applied to control the air temperature in the buildings. The SMC method is only one of the control methods used in home automation systems. In addition, other types of regulators are used to stabilise indoor air temperatures such as PI controller [10] or PID controls for the different control areas of the heating, ventilation, and air conditioning (HVAC) systems [11].

The main objectives of the paper are as follows:

1) Design a control law that forces the trajectory of the dynamic system from any initial condition to the sliding surface in finite time. After reaching the sliding surface, the trajectory of the system should remain on it.
2) Describe a general thermal model of the building. The model will be relatively simple but will incorporate the major features of heat transfer dynamics. The parameters of the model will be easily estimated already at the design stage of the building. The model will be prepared in a form that allows simulating the indoor temperature dynamics in every room of the building.

The modelling approach, which is used in this paper, is based on the well-known heat conduction equation presented by Joseph Fourier in 1822 [12]. The mathematical theory of heat conduction has been the topic of a great number of publications, textbooks and monographs, such as [13] or [14] which present a very detailed analysis of heat transfer aspects. A systematic review of the historical development of mathematical models applied in the development of building technology can be found in articles [15, 16]. The review with the references given therein provides an insight into various modelling approaches, including physical modelling, neural networks, expert systems, fuzzy logic and genetic models.

The physical phenomena of thermal conductivity are very complex and usually described by non-linear partial differential equations. These equations also depend on time and space variables. For these reasons, it is extremely difficult to obtain a single complete thermal model of a building. Conversely, the mathematical model is crucial in the design process for control algorithms. In the literature, we distinguish three methods frequently used to obtain and identify an approximated thermal model of a building. The first method is called *the impulse response method* [17, 18]. It is based on the output response of the model if the excitation of input is a unit impulse. Under additional assumptions and with the help of the Laplace transform, the output response of the wall to unit impulse excitation function can be expressed as a time series.

The second method is *the finite difference method.* This is a numerical method for solving partial differential equations of heat conduction [17, 18]. The finite difference method is based on the approximation of derivatives by algebraic equations. The building wall is divided into a finite number of layers, and temperature for each layer is computed using a set of algebraic equations.

The third method is known as *the lumped parameter method* (or *the lumped capacitance method*). This method is based on the assumption that the transfer of the heat flux between two spaces, which are divided by a partition (wall), can be modelled by the equivalent electrical RC circuit [19, 20]. Resistances in the electrical RC circuit are interpreted as thermal resistances; capacitances are interpreted as heat capacities of the modelled elements. The physical properties of the construction materials of the building are represented by resistors and capacitors. The lumped parameter method describes changes in air temperature at one (*lumped*) point. The mathematical model, which is obtained by using the lumped parameter method, takes the form of linear differential equations and can be simplified by the reduction of the number of states which are unobservable [23]. The model can be then easily solved by analytical or numerical methods. In this paper, a certain modification of the lumped parameter method is applied in order to obtain a model of the building that can be used for the design of the sliding mode controller.

The mathematical models of dynamic systems in the form of linear differential equations with integer-order derivatives can be expanded to models in the form of differential equations with fractional-order derivatives. Lower prices of computers and their increasing computing capacities enable to use frac tional-order calculus in practical solutions. More information about using fractional-order calculus for the modelling of heat transfer processes can be found in [24] where authors presents results of modeling the heat transfer in media and with assumption that heat flux is dispersed. The paper [25] presents how to implement non-integer order calculus to model one-dimensional heat transfer process with the use of Caputo-Fabrizio operator. Practical confirmation of the usefulness of fractional calculus for modeling dynamic changes in air temperature can be found in [26]. The current paper is organised as follows. In the next section, a general mathematical model for the temperature dynamics in buildings is introduced. In Subsec. 2.2, the design process for the sliding mode controller is described. The following section applies the concept to an exemplary building structure consisting of five rooms. Conclusions are presented in Sec. 4.

2. Methodology

2.1. Model description

A typical building can be considered as a collection of rooms arranged in a specific order, with each room enclosed by walls, floor, and ceiling. A single room usually has several windows and is accessible via doors. Let $i \in \{1, 2, \dots, n\}$ be the index of a room in the sample building. Let us assume that the indoor air temperature in T_i in i-th room with volume V_i is uniform. Let us denote by Q_i^{out} the thermal power which is transferred out of the room (i.e., dissipated thermal power) and by Q_i^{in} the thermal power which is transferred into the room (i.e., external source of heat). Then, the temperature dynamics in the i-th room can be described by the following equation:

$$c\rho V_i \frac{\mathrm{d}T_i}{\mathrm{d}t} = Q_i^{\mathrm{in}}(t) - Q_i^{\mathrm{out}}(t), \qquad T_i(0) = T_i^0, \tag{2.1}$$

where ρ is the density of air, c is the specific heat capacity of air, and T_i^0 is the initial temperature, $t > 0$.

In this paper, the applied thermal power Q_i^{in} will denote the heat transferred to the air through a radiator or other radiant heating devices. More generally, the applied thermal power will consider, in addition, the heat from solar radiation, as well as the heat from occupants, lights, equipment and machinery. For simplification purposes, these heat gains are omitted from further analysis.

The overall thermal power loss from a room can be described as follows:

$$Q_i^{\mathrm{out}}(t) = Q_i^{\mathrm{tc}}(t) + Q_i^{\mathrm{ve}}(t), \tag{2.2}$$

where Q_i^{tc} refers to heat loss by thermal conduction through doors, walls, ceiling, windows etc., and Q_i^{ve} refers to heat loss by ventilation.

Heat loss by thermal conduction can be expressed as (e.g. [27])

$$Q_i^{\mathrm{tc}}(t) = \sum_{j=-1}^{n} A_{i,j} U_{i,j} (T_i(t) - T_j(t)), \tag{2.3}$$

where $U_{i,j}$ is the resultant overall heat transfer coefficient that corresponds to $A_{i,j}$, $A_{i,j}$ is the area of exposed surface between i-th and j-th room, the room indexed as $j = 0$ stands for the outer space, and $j = -1$ stands for the earth. The resultant heat transfer coefficient $U_{i,j}$ can be calculated as a weighted average of the elements that the surface $A_{i,j}$ is composed of, that is [28]

$$U_{i,j} = \frac{\sum\limits_k A_{i,j,k} U_{i,j,k}}{\sum\limits_k A_{i,j,k}}, \tag{2.4}$$

where $\sum\limits_k A_{i,j,k} = A_{i,j}$.

The loss of heat due to ventilation with heat recovery can be expressed as (e.g. [29])

$$Q_i^{\mathrm{ve}}(t) = (1-\beta)c\rho q_i \left(T_i(t) - T_0(t)\right), \tag{2.5}$$

where q_i denotes air volume flow, and β stands for heat recovery efficiency.

Finally, the model of the air temperature dynamics in the building can be expressed by Eqs (2.1)–(2.5) and written using the state space notation in the following form:

$$\mathbf{E}\dot{\mathbf{x}}(t) = \mathbf{A}\mathbf{x}(t) + \mathbf{B}\mathbf{u}(t) + \mathbf{Z}\mathbf{z}(t), \qquad \mathbf{x}(0) = \mathbf{x}_0, \tag{2.6}$$

where

$$\mathbf{x}(t) = [x_1(t)\ x_2(t)\ ...\ x_n(t)]^{\mathrm{T}} \in \mathbb{R}^n, \quad x_i(t) = T_i(t), \qquad i = 1,2,...,n, \tag{2.7}$$

$$\mathbf{u}(t) = [u_1(t)\ u_2(t)\ ...\ u_n(t)]^{\mathrm{T}} \in \mathbb{R}^n, \quad u_i(t) = Q_i^{\mathrm{in}}(t), \qquad i = 1,2,...,n, \tag{2.8}$$

$$\begin{gathered} \mathbf{z}(t) = [z_1(t)\ z_2(t)]^{\mathrm{T}} \in \mathbb{R}^2, \qquad z_1(t) = T_0(t), \quad z_2(t) = T_{-1}(t), \\ t > 0, \quad \mathbf{x}_0 \in \mathbb{R}^n, \end{gathered} \tag{2.9}$$

$$\mathbf{E} = c\rho\,\mathrm{diag}(V_1, V_2, ..., V_n), \tag{2.10}$$

$$\mathbf{A} = \begin{bmatrix} -\sum\limits_{j=1}^n A_{1,j}U_{1,j} & A_{1,2}U_{1,2} & \dots & A_{1,n}U_{1,n} \\ A_{2,1}U_{2,1} & -\sum\limits_{j=1}^n A_{2,j}U_{2,j} & \dots & A_{2,n}U_{2,n} \\ \vdots & \vdots & \ddots & \vdots \\ A_{n,1}U_{n,1} & A_{n,2}U_{n,2} & \dots & -\sum\limits_{j=1}^n A_{n,j}U_{n,j} \end{bmatrix} - (1-\beta)c\rho \begin{bmatrix} q_1 \\ q_2 \\ \vdots \\ q_n \end{bmatrix} \mathbf{I}_n, \tag{2.11}$$

$$\mathbf{B} = \mathrm{diag}(b_1, b_2, ..., b_n), \tag{2.12}$$

(2.13) $$b_i = \begin{cases} 1, & \text{if } i\text{-th room is equipped with a heating device,} \\ 0, & \text{otherwise,} \end{cases}$$

(2.14) $$\mathbf{Z} = \begin{bmatrix} A_{1,0}U_{1,0} + (1-\beta)c\rho q_1 & A_{1,-1}U_{1,-1} \\ A_{2,0}U_{2,0} + (1-\beta)c\rho q_2 & A_{2,-1}U_{2,-1} \\ \vdots & \vdots \\ A_{n,0}U_{n,0} + (1-\beta)c\rho q_n & A_{n,-1}U_{n,-1} \end{bmatrix}.$$

The output equations of the state space representation are based on the measurement of sensors that relate to the air temperature in the rooms

(2.15) $$\mathbf{y}(t) = \mathbf{C}\mathbf{x}(t),$$

where

(2.16) $$\mathbf{y}(t) = [y_1(t)\ y_2(t)\ ...\ y_n(t)]^{\mathrm{T}} \in \mathbb{R}^n, \qquad y_i(t) = T_i(t), \qquad i = 1, 2, ..., n,$$

(2.17) $$\mathbf{C} = \mathrm{diag}(c_1, c_2, ..., c_n),$$

(2.18) $$c_i = \begin{cases} 1, & \text{if } i\text{-th room is equipped with a temperature sensor,} \\ 0, & \text{otherwise.} \end{cases}$$

2.2. Synthesis of a sliding mode controller

We consider the situation where every room is equipped with a heating device, which means that $\mathbf{B} = \mathbf{I}_n$. We also assume that in every room a sensor measures indoor temperature, therefore, $\mathbf{y}(t) = \mathbf{x}(t)$. Under these assumptions, we can define the sliding surface for the system (2.6), (2.15) in the following form:

(2.19) $$\mathbf{s}(t) = \mathbf{x}(t) - \mathbf{x}_{\mathrm{d}}(t),$$

where $\mathbf{x}_{\mathrm{d}}(t)$ is the desired trajectory. The problem is to find a control law that guarantees the existence of the sliding mode around the defined surface (2.19).

Let us consider the following formula:

(2.20) $$\mathbf{u}(t) = -\mathbf{B}^{-1}\left(\mathbf{A}\mathbf{x}(t) - \mathbf{E}\dot{\mathbf{x}}_{\mathrm{d}}(t)\right) - \mathbf{B}^{-1}\mathbf{S}(t)\mathbf{z}^{\max} - \sigma\mathbf{B}^{-1}\mathbf{S}(t)\mathbf{s}_\eta(t) - \gamma\mathbf{B}^{-1}\mathbf{s}(t),$$

where $\sigma > 0$, $\gamma > 0$ are positive coefficients, and $\mathbf{z}^{\max} \in \mathbb{R}^n$ is a vector whose elements are the upper bounds of the corresponding elements of $\mathbf{Zz}(t)$, that is

$$\mathbf{z}^{\max} = \max_{t \geq 0} \mathbf{Zz}(t) \geq \mathbf{0}, \tag{2.21}$$

$$\mathbf{S}(t) = \mathrm{diag}\big(\mathrm{sgn}(s_1(t)), \mathrm{sgn}(s_2(t)), ..., \mathrm{sgn}(s_n(t))\big), \tag{2.22}$$

$$\mathbf{s}_\eta(t) = \big[|s_1(t)|^\eta \ \ |s_2(t)|^\eta \ \ ... \ \ |s_n(t)|^\eta\big]^{\mathrm{T}}, \tag{2.23}$$

η is a ratio of two odd positive integers satisfying $0 < \eta < 1$.

Theorem 2.1. The trajectory of the system (2.6) is forced by the control (2.8) from any initial condition to the surface (2.19) in finite time and, then, remains on it.

Proof. The proof is approached by imposing the following Lypunov function:

$$V(t) = 0.5\mathbf{s}(t)^{\mathrm{T}}\mathbf{s}(t). \tag{2.24}$$

The derivative of the functional V with respect to time t and along the solutions of the system (2.6) becomes

$$\begin{aligned} \dot{V}(t) &= \mathbf{s}(t)^{\mathrm{T}}\dot{\mathbf{s}}(t) = \mathbf{s}(t)^{\mathrm{T}}\left(\dot{\mathbf{x}}(t) - \dot{\mathbf{x}}_{\mathrm{d}}(t)\right) \\ &= \mathbf{s}(t)^{\mathrm{T}}\left(\mathbf{E}^{-1}\mathbf{Ax}(t) + \mathbf{E}^{-1}\mathbf{Bu}(t) + \mathbf{E}^{-1}\mathbf{Zz}(t) - \dot{\mathbf{x}}_{\mathrm{d}}(t)\right). \end{aligned} \tag{2.25}$$

Substitution of (2.20) by (2.25) yields

$$\begin{aligned} \dot{V}(t) = &-\mathbf{s}(t)^{\mathrm{T}}\mathbf{E}^{-1}\mathbf{S}(t)\mathbf{z}^{\max} - \mathbf{s}(t)^{\mathrm{T}}\mathbf{E}^{-1}\sigma\mathbf{S}(t)\mathbf{s}_\eta(t) \\ &- \mathbf{s}(t)^{\mathrm{T}}\mathbf{E}^{-1}\gamma\mathbf{s}(t) + \mathbf{s}(t)^{\mathrm{T}}\mathbf{E}^{-1}\mathbf{Zz}(t). \end{aligned} \tag{2.26}$$

From (2.21) it follows that

$$\begin{aligned} \dot{V}(t) &\leq -\gamma\lambda_{\min}(\mathbf{E}^{-1})\left\|\mathbf{s}(t)\right\|^2 - \sigma\lambda_{\min}(\mathbf{E}^{-1})\left\|\mathbf{s}(t)\right\|^{\eta+1} \\ &= -2\gamma\lambda_{\min}(\mathbf{E}^{-1})V(t) - 2^{\frac{\eta+1}{2}}\sigma\lambda_{\min}(\mathbf{E}^{-1})V(t)^{\frac{\eta+1}{2}}. \end{aligned} \tag{2.27}$$

By taking $\alpha = 2\gamma\lambda_{\min}(\mathbf{E}^{-1}) > 0$, $\beta = 2^{\frac{\eta+1}{2}}\sigma\lambda_{\min}(\mathbf{E}^{-1}) > 0$, $\kappa = \frac{\eta+1}{2}$ it can be concluded from Lemma 2.1 that the system state will reach the sliding mode surface in finite time calculated as follows:

$$t_r = \frac{1}{\alpha(1-\kappa)} \ln \frac{\alpha V(0)^{1-\kappa} + \beta}{\beta}, \tag{2.28}$$

where

$$V(0) = 0.5\mathbf{s}(0)^{\mathrm{T}}\mathbf{s}(0). \tag{2.29}$$

□

Lemma 2.1 ([9, 30]). Assuming that a continuous positive-definite function $V(t)$ satisfies the following differential inequality

$$\dot{V}(t) \leq -\alpha V(t) - \beta V(t)^{\kappa}, \quad \forall_{t \geq t_0},\ V(t_0) \geq 0, \tag{2.30}$$

where α and β are positive constants, and κ is a ratio of two odd positive integers, such as $0 < \kappa < 1$. Then, for any given time t_0, $V(t)$ converges to zero at least within a finite time

$$t_r = t_0 + \frac{1}{\alpha(1-\kappa)} \ln \frac{\alpha V(t_0)^{1-\kappa} + \beta}{\beta}. \tag{2.31}$$

Proof. The proof of this lemma can be found in [9].

□

3. Case study

We consider a single-family house, see Figs 1 and 2. The house consists of five rooms, including bedroom, living-room, bathroom, kitchen, and anteroom, see Table 1.

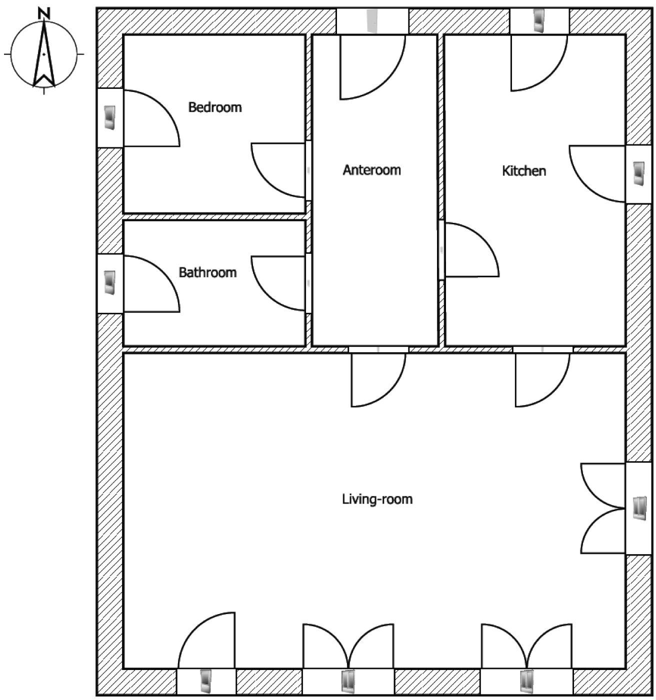

Fig. 1. Floor plan of the house.

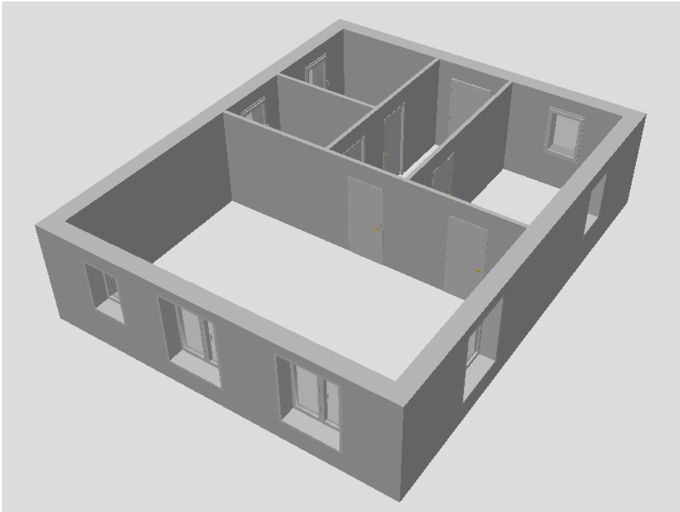

FIG. 2. 3D projection of the house.

Table 1. List of rooms with associated indexes. Earth and outer space are also considered as rooms with special indexes: −1 and 0 respectively.

Room name	Earth	Outer space	Bedroom	Bathroom	Living-room	Kitchen	Anteroom
Index	−1	0	1	2	3	4	5

The outer walls have a thickness of 47 cm and are built with four layers: structural clay tile (30 cm), mineral wool as an insulating material (15 cm), and internal (1 cm) and external (1 cm) cement-lime plasters. The internal walls have a thickness of 12 cm and are made of brick (10 cm) with 1 cm cement-lime plaster on both sides. The roof is isolated with mineral wool of 20 cm thickness. The building construction elements and geometry parameters are presented in Tables 2–5. The house is equipped with a heat recovery system (with an efficiency of 80%) and mechanical ventilation. It was assumed that air volume flow is constant for each room. The parameters of the ventilation system are summarised in Table 4.

Table 2. Areas of the surfaces between separated zones.

$A_{i,j}$ [m^2]	−1	0	1	2	3	4	5
1	7.51	21.18	0	6.90	0	0	6.77
2	5.31	10.11	6.90	0	6.90	0	4.80
3	36.43	79.36	0	6.90	0	6.87	4.75
4	13.02	31.07	0	0	6.87	0	11.8
5	9.39	14.14	6.77	4.80	4.75	11.8	0

Table 3. Resultant overall heat transfer coefficients corresponding to the surfaces $A_{i,j}$.

$U_{i,j}$ [W/(m$^2\cdot$K)]	−1	0	1	2	3	4	5
1	0.30	0.27	0	0.80	0	0	1.00
2	0.30	0.30	0.80	0	0.8	0	1.08
3	0.30	0.30	0	0.80	0	0.99	1.08
4	0.30	0.28	0	0	0.99	0	0.91
5	0.30	0.34	1.00	1.08	1.08	0.91	0

Table 4. Volumes of rooms and ventilation rates.

	1	2	3	4	5
V_i, [m^3]	18.78	13.28	91.08	32.55	23.48
q_i [m^3/h]	20	50	60	70	10

Table 5. Other building geometry parameters and thermal properties of building construction elements.

Parameter	Symbol	Value	Unit
Specific heat capacity of air	c	1005	J/(kg·K)
Density of air	ρ	1.205	kg/m^3
Heat recovery efficiency	β	0.8	–
Surface area of exterior doors	$A_{i,j,k}$	2.31	m^2
Surface area of interior doors	$A_{i,j,k}$	1.89	m^2
Surface area of a single window	$A_{i,j,k}$	1.17	m^2
Surface area of a double window	$A_{i,j,k}$	2.52	m^2
Overall heat transfer coefficient of exterior doors	$U_{i,j,k}$	0.25	W/(m$^2\cdot$K)
Overall heat transfer coefficient of interior doors	$U_{i,j,k}$	0.8	W/(m$^2\cdot$K)
Overall heat transfer coefficient of a window	$U_{i,j,k}$	0.9	W/(m$^2\cdot$K)

The house is equipped with a central heating system, whereby every room has its own radiator. A thermostat unit is mounted on every radiator controlling the flow of hot central heating water into the radiator. We assume that all radiators in the house can be controlled by a central unit that implements a control algorithm. The outdoor air and earth temperatures are measured using external sensors. In addition, every room is equipped with a sensor that measures indoor temperature.

The dynamics of the indoor air temperature can be described by Eq. (2.6) with $n = 5$. The earth temperature is assumed to be stable at a level of 15.0°C. The daily profile of the outside temperature that has been used in the simulation experiments is presented in Fig. 3. The desired temperature profile for every room is defined by the following function:

$$x_{\mathrm{d}i}(t) = -2\cos\left(\frac{2\pi}{24}(t-4)\right) + 20, \qquad i = 1, 2, ..., 5. \tag{3.1}$$

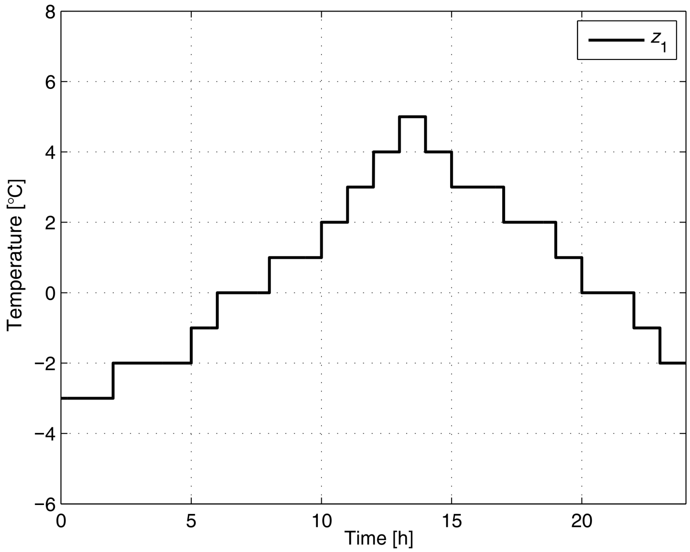

FIG. 3. Outdoor air temperature over the course of the simulation experiment.

The temperature (3.1) is given in Celsius, as well as the initial condition

$$\mathbf{x}(0) = [15.0 \;\; 16.0 \;\; 17.0 \;\; 15.0 \;\; 14.0]^{\mathrm{T}}.$$

The central unit implements the sliding mode control algorithm (2.20) with the following parameters:

$$\sigma = 100, \qquad \gamma = 10^6, \qquad \eta = 3/5,$$
$$\mathbf{z}^{\max} = 10^7 \cdot [1.003 \;\; 0.608 \;\; 4.397 \;\; 1.627 \;\; 0.982]^{\mathrm{T}}.$$

Every element of the vector $\mathbf{z}^{\max}$ represents heat power expressed in watts. In addition, we take into consideration the following constraints imposed by the radiator construction:

$$0\,[\mathrm{W}] \le u_1(t) \le 500\,[\mathrm{W}], \tag{3.2}$$

$$0\,[\mathrm{W}] \le u_2(t) \le 500\,[\mathrm{W}], \tag{3.3}$$

$$0\,[\mathrm{W}] \le u_3(t) \le 3000\,[\mathrm{W}], \tag{3.4}$$

$$0\,[\mathrm{W}] \le u_4(t) \le 800\,[\mathrm{W}], \tag{3.5}$$

$$0\,[\mathrm{W}] \le u_5(t) \le 400\,[\mathrm{W}]. \tag{3.6}$$

The sample simulation results are presented in Figs 4 and 5. The upper plots show temperatures change during the whole simulation and the bottom plots show temperatures change in the zoomed time window. As can be noticed, at the be-

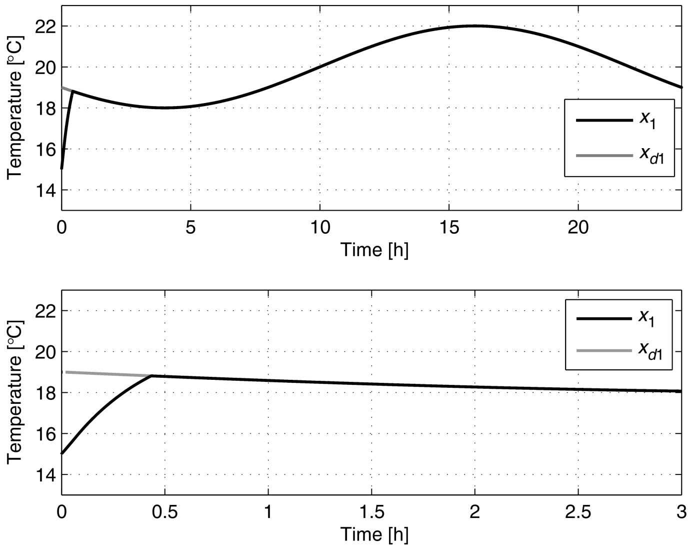

FIG. 4. The trajectory x_1 (black line) of the closed-loop system with the sliding mode controller and the desired trajectory $x_{\mathrm{d}1}$ (grey line). The trajectory x_1 represents the indoor temperature in the bedroom. The same simulation results are shown in different time windows.

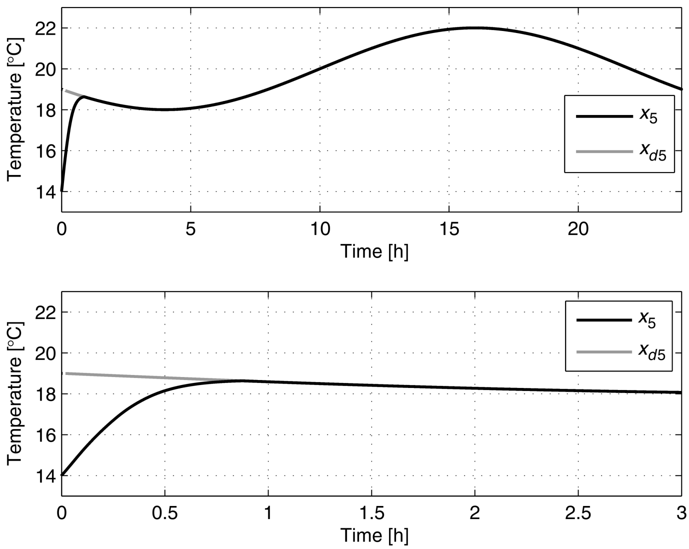

FIG. 5. The trajectory x_5 (black line) of the closed-loop system with the sliding mode controller and the desired trajectory $x_{\mathrm{d}5}$ (grey line). The trajectory x_5 represents the indoor temperature in the anteroom. The same simulation results are shown in different time windows.

ginning of the simulation the indoor air temperature changes faster until the desired temperature is reached. When this happens, the internal air temperature changes according to the desired temperature, despite external disturbances, such as the outside temperature. Figure 5 shows the air temperature changes in the anteroom. It can be noticed that this temperature changes slowly before it reaches the desired temperature $x_{\mathrm{d}5}(t)$. This is due to the fact that the anteroom has relatively the smallest radiator.

4. Conclusions

An efficient and practical way for modelling heat transfer dynamics in a building, which can be an office area, apartment house, industrial plant etc., was presented in this paper. The resulting mathematical model is represented by first-order differential equations. The number of rooms where the indoor air temperature is controlled determines the order of the dynamical model. The presented modelling approach allows the incorporation of to incorporate various forms of heat loss and heat gain. One of the main advantages of the such modelling approach is that the model parameters can be determined easily and uniquely from the geometry of the building and the thermal properties of the building materials. As a result, the formal identification of the model parameters is not required. This approach leads to mathematical models that can be used for the design of temperature control algorithms. In this paper, a proposed sliding mode controller guarantees the existence of the sliding mode around the defined sliding surface. The trajectory of the closed-loop system reaches the sliding surface after a finite time and, then, remains on it. The simulation example has shown the effectiveness of the proposed method. Numerical calculations and computer simulations were performed in the MathWorks™ MATLAB®/Simulink® environment.

References

1. Edward C., Spurgeon S., *Sliding mode control: theory and appliations*, Taylor and Francis, London, 1998.
2. Pisano A., Usai E., *Sliding mode control: a survey with application in math*, Mathematics and Computers in Simulation, **81**(5): 954–979, 2011.
3. Długosz M., *Optimization problems of power transmission in automation and robotics*, Przeglad Elektrotechniczny, **87**(9A): 238–242, 2011.
4. Abid M., Mansouri A., Aissaoui A., Belabbes B., *Sliding mode application in position control of an induction machine*, Journal of Electrical Engineering, **59**(6): 322–327, 2008.
5. Perić S.L., Antić D.S., Nikolić V.D., Mitić D.B., Milojković M.T., Nikolić S.S., *A new approach to the sliding mode control design: anti–lock braking system as a case study*, Journal of Electrical Engineering, **65**(1): 37–43, 2014.

6. Bandyopadhyay B., Deepak F., Kim K.S., *Sliding mode control using novel sliding surfaces*, Springer-Verlag, Berlin, Heidelberg, 2010.

7. Liu J., Sun F., *A novel dynamic terminal sliding mode control of uncertain nonlinear systems*, Journal of Control Theory and Applications, **5**(2): 189–193, 2007.

8. Man Z., Yu X.H., *Terminal sliding mode control of MIMO linear systems*, IEEE Transactions on Circuits and Systems I: Fundamental Theory and Applications, **44**(11): 1065–1070, 1997.

9. Mobayen S., Majd V.J., Sojoodi M., *An LMI-based composite nonlinear feedback terminal sliding-mode controller design for disturbed MIMO systems*, Mathematics and Computers in Simulation, **85**(11): 1–10, 2012.

10. Kulkarni M.R., Hong F., *Energy optimal control of a residential space-conditioning system based on sensible heat transfer modeling*, Building and Environment, **39**(1): 31–38, 2004.

11. Blasco C., Monreal J., Benítez I., Lluna A., *Modelling and PID control of HVAC system according to energy efficiency and comfort criteria*, [in:] *Sustainability in Energy and Buildings*, N. M'Sirdi, A. Namaane, R.J. Howlett, L.C. Jain (Eds), pp. 365–374, Springer, Berlin, Heidelberg, 2012.

12. Fourier J., *The analytical theory of heat*, Dover Publicatons, Inc., New York, USA, 1955.

13. Jakob M., *Heat transfer*, John Willey & Sons, New York, USA, 1949.

14. Gröber H., Erk S., *Fundamentals of Heat Transfer*, McGraw-Hill, 1961.

15. Lu X., Clements-Croome D., Viljanen M., *Past, present and future mathematical models for buildings: focus on intelligent buildings (part 1)*, Intelligent Buildings International, **1**(1): 23–38, 2009.

16. Lu X., Clements-Croome D., Viljanen M., *Past, present and future mathematical models for buildings: focus on intelligent buildings (part 2)*, Intelligent Buildings International, **1**(2):131–141, 2009.

17. Clarke J., *Energy simulation in building design*, Butterworth Heinemann, Woburn, USA, 2001.

18. Underwood C.P., Yik F., *Modelling methods for energy in buildings*, Blackwell Science, Oxford, United Kingdom, 2004.

19. Gouda M.M., Danaher S., Underwood C.P., *Low-order model for the simulation of a building and its heating system*, Building Services Engineering Research and Technology, **21**(3): 199–208, 2000.

20. Gouda M.M., Danaher S., Underwood C.P., *Building thermal model reduction using nonlinear constrained optimization*, Building and Environment, **37**(12): 1255–1265, 2002.

21. Bergman T.L., Incropera F.P., DeWitt D.P., Lavine A.S., *Fundamentals of heat and mass transfer*, John Wiley & Sons, 2011.

22. Davies M.G., *Building Heat Transfer*, John Wiley & Sons, 2004.

23. Długosz M., *Aggregation of state variables in an RC model*, Building Services Engineering Research and Technology, **39**(1): 66–80, 2018.

24. Sierociuk D., Dzieliński A., Sarwas G., Petras I., Podlubny I., Skovranek T., *Modelling heat transfer in heterogeneous media using fractional calculus*, Philosophical Transactions of the Royal Society A: Mathematical, Physical and Engineering Sciences, **371**(1990): 20120146, 2013.

25. Oprzędkiewicz K., *Non integer order, state space model of heat transfer process using Caputo-Fabrizio operator*, Bulletin of the Polish Academy of Sciences: Technical Sciences, **66**(3): 249–255, 2018, doi: 10.24425/122105.

26. Długosz M., Skruch P., *The application of fractional-order models for thermal process modelling inside buildings*, Journal of Building Physics, **39**(5): 440– 451, 2016.

27. Polish Committee for Standardization, *PN-EN ISO 13790:2009. Thermal performance of buildings – Calculation of energy use for space heating and cooling*, http://www.pkn.pl (accessed: August 29, 2012), 2009.

28. Polish Committee for Standardization,*PN-EN ISO 6946:2008. Building components and building elements. Thermal resistance and thermal transmittance – Calculation method*, http://www.pkn.pl (accessed: August 29, 2012), 2008.

29. Polish Committee for Standardization, *PN-B-03430:1983. Ventilation in dwelling and public utility buildings – Specifications*, http://www.pkn.pl (accessed: August 29, 2012), 1983.

30. Moulay E., Perruquetti W., *Finite time stability and stabilization of a class of continuous systems*, Journal of Mathematical Analysis and Applications, **323**(2): 1430–1443, 2006.

Received October 19, 2018; accepted version May 6, 2019.